

ESTIMATING AND ANALYZING THE STABILITY OF BRAZILIAN GNSS STATIONS FOR TECTONIC STUDIES

Yellinson de Moura Almeida ^{1*}, Giuliano Sant'Anna Marotta ,
João Francisco Galera Monico , Gabriela de Oliveira N. Brassarote ,
and George Sand Leão A. França 

¹Universidade de Brasília - UnB, Observatório Sismológico, Brasília, DF, Brazil

²Universidade Estadual Paulista - UNESP, Presidente Prudente, SP, Brazil

³Universidade de São Paulo - USP, Department of Geophysics, São Paulo, SP, Brazil

*Corresponding author: y.moura.almeida@gmail.com

ABSTRACT. The detailed study of stresses and strains is fundamental for geophysical and geodetic studies, enabling the development of plate motion models, geodynamic processes and several proposals. GNSS positioning has been used to estimate these stresses and strains. However, for the accuracy required, it is necessary a rigorous assessment of the behavior of GNSS stations and their position time series. This paper aims to analyze the influence of the different types of geodetic monuments present in the Brazilian GNSS Continuous Monitoring Network by estimating and characterizing noise in the time series and investigating variables that can affect the stability of the stations to establish criteria for using these data in tectonic and geodynamic studies. The evaluation of 119 GNSS stations throughout Brazil indicates the significant presence of random walk noise in some of these stations, detected by analyzing the magnitude of the noise and the spectral index. It was found that the stations with unstable monuments have been observed for at least eight years and are mostly in coastal areas or under the influence of large watercourses.

Keywords: time series analysis, geodetic monuments, noise characterization, geodynamic processes.

INTRODUCTION

The main components of the stresses acting on the South American Plate are generated by the ongoing subduction of the Nazca Plate and the formation of young crust on the mid-Atlantic ridge (Norabuena et al., 1998; Lima, 2000; Marotta et al., 2015; Rocha et al., 2016). Therefore, global stress models characterize the South American intraplate region according to these regional components (Assumpção et al., 2016). However, several studies have indicated the existence of stresses resulting from local rheological and structural features that can either potentially modify both the direction and magnitude or intensify the field of tectonic stresses, as well as affect significantly the observed deformations (Calais et al., 2006; Aguerto-Detzel et al., 2014; Assumpção et al., 2016; Yadav and Tiwari, 2018).

The detailed study of resulting stresses and deformations is fundamental for geophysical and geodetic

applications, as it allows modeling the movement of plates and geological blocks, crustal and mantle geodynamics processes while supporting climate change studies and the understanding of associated phenomena and processes (Kierulf et al., 2021).

In Brazil, several studies have raised essential hypotheses and observations regarding the field of stresses. Aguerto-Detzel et al. (2014) highlighted the difficulty of characterizing stresses from seismological studies using focal mechanism, due to the low magnitude of intraplate seismic events. Assumpção et al. (2004), Barros et al. (2009), Chimiplaganond et al. (2010) and Rocha et al. (2016), among others, point to the crustal and lithospheric thinning of some regions, and the presence of sedimentary basins, pre-existing faults and other geological factors, as favorable for the concentration of stress.

GNSS positioning of the stations, where a position time series allows estimating motion and deformation

rates, has been widely used to improve the estimation and analysis of the above-mentioned processes and mechanisms (Marotta et al., 2013a,b, 2015) to assist in the understanding of regional tectonic and geodynamic processes. However, a more rigorous assessment of the behavior of GNSS stations and their position time series is essential to achieve the required accuracy.

To this end, while emphasizing Brazil, this work sought to analyze the influence of the different types of geodetic monuments present in the Brazilian GNSS Continuous Monitoring Network by estimating and characterizing the noise in the time series while investigating the variables that may affect the stability of GNSS stations, in order to establish criteria for using these data in tectonic and geodynamic studies.

It is noteworthy that, for the most part, RBMC stations were not designed for geotectonic studies, and it is essential to develop a strategy to identify stations whose levels of instability are incompatible with the desired application since surface processes also affect the GNSS time series and propagate to the velocity and deformation estimates.

Thus, the horizontal velocities for each of the GNSS stations were also estimated in this study in addition to the proposed analysis. These velocities allow dynamic monitoring of reference frames, evaluation of movements caused by seismic events, estimation of movements between tectonic plates and several other applications in geodesy (Sánchez and Drewes, 2020).

NOISE IN TIME SERIES OF GNSS SOLUTIONS

The use of the GNSS position time series for estimating a model that describes the motion of a geological plate or block requires that these series record both the phenomenon of interest and other phenomena. Therefore, defining a functional model that expresses the present phenomena and allows their differentiation should be considered.

Currently, Nikolaidis (2002), Cenni et al. (2012), and Farolfi and Ventisette (2015) have presented a well-accepted functional model (Equation 1) that considers the aforementioned phenomena:

$$y(t_i) = a + b(t_i - t_0) + \sum_{k=1}^2 \sin(2\pi k t_i + \phi_k) + \sum_{j=1}^J d_j H(t_j - t_i) + v_i, \quad (1)$$

where $y(t_i)$ represents the position observed at the point for each direction (n, e, u) at the time t_i ; a is the position at a time t_0 ; b is the speed for each direction (n, e, u); c_k are the annual and semi-annual amplitudes; ϕ_k are the phases; d_j is the discontinuity introduced at the time t_j ; H is the jump function, with $H(t_j - t_i) = 0$ if $t_i < t_j$ and $H(t_j - t_i) = 1$ if $t_i \geq t_j$; and v_i is the residue.

The model represented in Equation 1 can be estimated deterministically. However, since the residuals (v) can represent both unmodeled effects and errors associated with observations, they can affect the estimation of unknown parameters and their uncertainties. Therefore, if GNSS coordinate solutions are strongly correlated in time (Amagua et al., 2018), it will be necessary to use a stochastic method to estimate more realistic uncertainties of the estimated parameters.

In general, the estimated residuals can be considered stochastic noise and may be described either by a Power Law process (Mandelbrot, 1983; Agnew, 1992; Williams et al., 2004) or the behavior in the time domain expressed as

$$P_y = P_0 \left(\frac{f}{f_0} \right)^k, \quad (2)$$

where: f is temporal frequency; P_0 and f_0 are the normalization constants; and k is the spectral index, whose values vary in the interval $[-3, 1]$.

In Equation 2, noise levels can be analyzed regarding the index k , which allows for classifying the station noise according to the presence of fractional Brownian movement in the interval $-3 < k < -1$ and fractional Gaussian noise for $-1 < k < 1$, so that $k=0$ indicates classic white noise; $k=-1$ indicates fractal noise, or flicker; and $k=-2$ indicates random walk noise (Williams et al., 2004).

While white noise is associated with errors in observations and characteristics of the GNSS receiver hardware, flicker noise is associated with multipath (Dmitrieva et al., 2016) and a wide variety of dynamic processes, including the Earth's oscillation around its axis and uncertainties in the time measured by satellites and receivers, in addition to atmospheric effects (Williams et al., 2004). Also, according to Williams et al. (2004), the random walk noise is mainly associated with the instability of the geodetic monument due to the changing conditions at the placement site, whether placed on soil, rock, building roofs etc. In this same study, the authors analyzed eight different types of geodetic monuments, from those anchored in the basement to those installed on concrete slabs on the roof and directly on the ground, and reported that stations installed on concrete pillars on the ground only performed better than stations installed on oil platforms, which are susceptible to a wide variety of movements.

It is observed that random walk is a type of non-stationary noise; thus, its characterization does not allow future prediction. Its detection in time series depends on the amount of data, sampling frequency and amplitudes relative to other types of noise, among other factors. Also, the instability of the geodetic

monument can be minimized using carefully designed structures anchored in a rocky basement, decoupled from the surface and counterbalanced regarding the winds (Wyatt, 1989; Bock et al., 1997).

Despite the above, the RBMC stations are mostly located on concrete roofs of public buildings and concrete pillars in the ground (Table 1), prioritizing longevity, security and the infrastructure (electricity and internet) necessary for the uninterrupted operation of the equipment. Amagua et al. (2018) and Ramos et al. (2022) reported that, compared to the other types of noise, the RBMC stations have significant white noise levels, although the white noise and flicker combination best describes the noise observed in these stations.

Note that using a single noise model for all stations has the great advantage of allowing comparing the noise characteristics of each station that is part of the same network, assuming that, up to a certain level, all stations are affected by the same noise sources and, therefore, have a similar power spectrum (Williams et al., 2004). However, it is suggested that different noise models should be considered depending on the application.

ESTIMATION OF VELOCITY MODELS BY THE WLS METHOD AND NOISE ANALYSIS BY MLE

Velocity models can be estimated by the Weighted Least Squares (WLS) method, using the functional model expressed by Equation 1, where the parameters are estimated using the time series of GNSS coordinates. Simultaneously, the type and amplitude of stochastic noises are evaluated based on the residuals. This assessment is usually conducted to provide the most realistic estimate of uncertainties for velocity models.

The Maximum Likelihood Estimation (MLE) of noise shows the need to maximize the likelihood function by adjusting the covariance (C) of the data. Thus, assuming a Gaussian distribution, the likelihood function (l) can be given as (Williams, 2008):

$$l(x, C) = \frac{1}{(2\pi)^{\frac{N}{2}} (\det C)^{\frac{1}{2}}} \exp(-0.5 \hat{v}^T C^{-1} \hat{v}), \quad (3)$$

$$\ln[l(x, C)] = -\frac{1}{2} [\ln(\det C) + \hat{v}^T C^{-1} \hat{v} + N \ln(2\pi)], \quad (4)$$

$$C = \sum_{i=1}^m \sigma_i^2 J_i, \quad (5)$$

where x is the vector of observed data; J , the covariance matrix for time-correlated noise, represented by a combination of different stochastic models; m is the number of stochastic models; \hat{v} , the vector of residuals; N , the number of observations; and σ^2 , the

variance of the stochastic model.

If the covariance matrix consists of a noise source, then we have:

$$C = \sigma^2 J, \quad (6)$$

$$\begin{aligned} \ln[l(x, \sigma)] = & -\frac{1}{2} [2N \ln(\sigma) + \ln(\det J) \\ & + \frac{\hat{v}^T J^{-1} \hat{v}}{\sigma^2} + N \ln(2\pi)], \end{aligned} \quad (7)$$

The considerations made allow us to assume that the estimated residuals and parameters (but not their uncertainties) do not change with a change of scale in the covariance matrix. In this case, Equation 7 can be derived regarding σ to find the value that provides maximum likelihood (Williams, 2008):

$$\sigma = \sqrt{\frac{\hat{v}^T J^{-1} \hat{v}}{N}}, \quad (8)$$

If the covariance matrix C depends on more than one noise source, it must be transformed. Therefore, when two noise sources are present, a two-dimensional covariance matrix should only need a one-dimensional numerical maximization. In this case, two noise amplitudes can be transformed into two alternative variables (an angle “ θ ” and a scalar “ r ”) and, for a given angle, it is possible to calculate a unit covariance matrix (C_{unit}) that describes the correct ratios of these two variables.

$$\sigma_1 = r \cos(\theta), \quad (9)$$

$$\sigma_2 = r \sin(\theta), \quad (10)$$

$$C_{unit} = r^2 [\cos^2(\theta) J_1 = \sin^2(\theta) J_2], \quad (11)$$

THE INFLUENCE OF DIFFERENT TYPES OF GEODETIC MONUMENTS PRESENT IN THE RBMC

This study used the daily time series solutions from 119 active stations of the Brazilian GNSS Continuous Monitoring available at the Nevada Geodetic Laboratory (NGL; (Blewitt et al., 2018); Figure 1). These solutions, which make up the time series of station coordinates, were referenced to IGS14 and estimated using the Precise Point Positioning method available in the GipsyX software, developed by the Jet Propulsion Laboratory of the California Institute of Technology.

The observation time of the selected stations is equal to or greater than 3 years (Figure 1), since observation periods shorter than three years may not show the effects to be modeled, according to Blewitt and Lavallée (2002) and Calais et al. (2006).

In addition to the daily solutions, the steps identified in the stations were included in the modeling of

Table 1: Types of monuments present in the RBMC of the studied GNSS stations.

Type of monument	Number of stations
Concrete pillar in building roof	58
Concrete pillar in the ground	40
Pillar in building structural column	7
Metallic tower in building roof	7
Others	7

the time series (Equation 1). The steps (Figure 1) correspond to events where the station position may have changed suddenly due to a change of either antenna or receiver, a seismic event and any other factor that may interfere with the recording of the station position, such as changes in the software. However, steps only concern events where the source of the change in station position is known.

The noise observed in the time series of the selected GNSS stations was estimated and analyzed using the software CATS (Create and Analyze Time Series), developed by [Williams \(2008\)](#). This software allows both estimating and comparing stochastic noise processes in a continuous time series, using MLE analysis, as well as calculating the spectral index k of the time series through periodic position solutions.

In addition to the noise analysis, the speeds and uncertainties for the selected stations were estimated by the WLS method, using different noise models and combining the entire spectral indices. This approach is recommended for large networks of GNSS stations, where the combination of white noise and flicker (WN+FN) or white noise and random walk (WN+RW) is considered adequate to describe the noise present in most stations.

Finally, assuming no pre-established noise magnitude limit to characterize the instability of a station, a criterion was established for classifying a station as unstable regarding the monumentation or nontectonic effects. To this, the spectral index k was analyzed for each component at each station and the amplitude of the WN+RW noise was analyzed using the GESD (Generalized Extreme Studentized Deviation) statistical test, proposed by [Rosner \(1983\)](#), traditionally used to identify outliers.

The GESD ([Rosner, 1983](#)) used in this work is commonly applied to samples with approximately normal distribution, where it is necessary to define a limit R of possible outliers. In this study, any component of a GNSS station that presents a WN+RW noise amplitude greater than that defined by the statistical test was considered an outlier and, therefore, unstable compared to the other stations on the network. After defining the criteria, R tests are performed separately: one test for one outlier, one test for two outliers, and up to R outliers. The test null

hypothesis is that there are no outliers in the sample. The alternative hypothesis is that there are up to r outliers.

$$R_i = \max \frac{x_i - \bar{x}V}{s}, \quad (12)$$

\bar{x} and s are the mean and the standard deviation of the samples, respectively. The test was performed for each component of each station, at 95% confidence level. After calculating the first R statistic, with all observations, the observation that maximizes $x_i - \bar{x}V$ is removed and the test is performed again with $n-1$ observations until R tests are performed. The critical values for each test are calculated by the following equation:

$$\lambda_i = \frac{(n-i)t_{p,n-i-1}}{\sqrt{(n-i-1+t_{p,n-i-1}^2)(n-i+1)}} \quad i = 1, 2, \dots, r, \quad (13)$$

where $t_{p,n-i-1}$ is the percentage of the t distribution for $n-i-1$ degrees of freedom; and p is:

$$p = 1 - \frac{\alpha}{2(n-i+1)}, \quad (14)$$

where α is the test significance level. Finally, the number of outliers is defined by finding the largest i , such that $R_i > \lambda_i$.

RESULTS AND DISCUSSION

Figure 2 presents the spectral index in the north, east and vertical components (n, e and u) for the GNSS stations studied. The average spectral index of the set of stations is $k = -0.67$, $k = -0.64$ and $k = -0.60$ for the n, e and u components, respectively.

These results corroborate the conclusion that the combination of white noise and flicker best describes the noise of the set of RBMC stations as reported by [Amagua et al. \(2018\)](#) and [Ramos et al. \(2022\)](#). However, indices $k < -1$ observed in the results (Figure 2) are further evidence that the random walk is also significantly present in some stations in the network.

The stations BEPA, BRFT, SALU and SMAR, with $k < -1$, correspond to approximately 3% of the total. The noise amplitudes in these stations

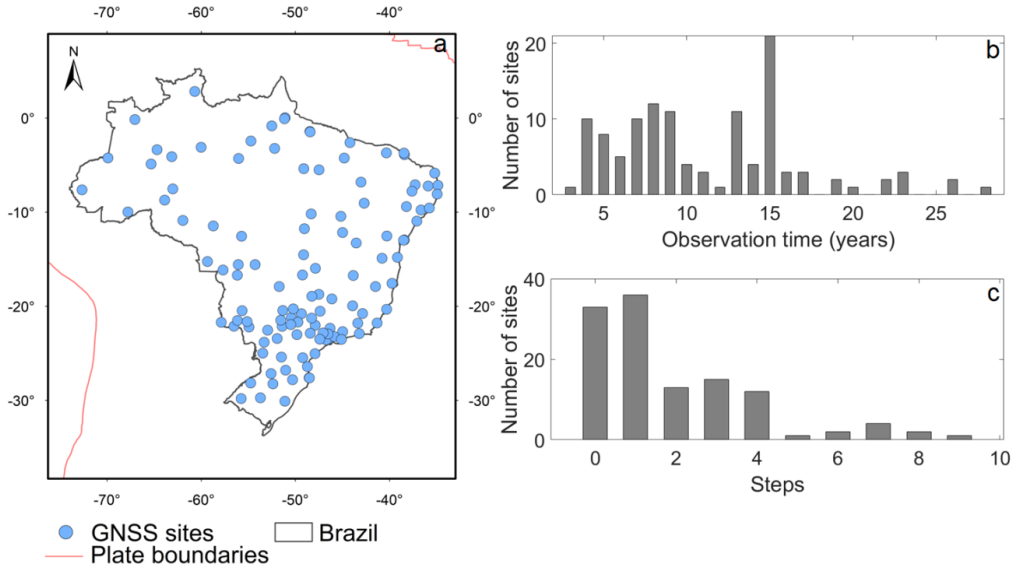


Figure 1: (a) Stations of the Brazilian GNSS Continuous Monitoring. (b) observation time of the GNSS stations. (c) number of steps observed in the stations.

are higher for the WN+RW model compared to the WN+FN model (Table 2). However, it is understood that the uncertainties determined by the WN+RW model are more realistic considering the influence of the random walk on the time series. Of the stations mentioned, BEPA, SALU and SMAR presented index $k < -1$ in the north and east components, thus highlighting the correlation between the horizontal components.

The GESD test was applied to the 119 stations studied to identify instability. The maximum number of supposed outliers was defined at 20% of the total stations ($R = 24$). If the calculated number of outliers is below this value, the test is complete. The statistical analysis was consistent since the number of outliers in each component was significantly below the number of tests performed. A total of 10 stations were classified as unstable since at least one component of the noise amplitude was an outlier (Table 3). Of these, BEPA, SALU and SMAR had already been classified as unstable because the northern and eastern components of the spectral index were lower than -1. Of the 10 stations, 6 were identified as outliers in the northern components; 7, in the eastern component; and 3, in the vertical component (Table 3).

Soil contraction, compaction of aquifer systems, gravity-driven downward movements, pore-elastic effects and monument deformation by thermal expansion or contraction are just a few examples of unmodeled factors that can influence the estimation of realistic uncertainties of GNSS velocities (Galloway and Jones, 1999; Calais et al., 2006; Ferreira et al., 2019). Therefore, the strategy of using a combination of WN+FN for all stations, after removing those where the magnitude of WN+RW is classified as discrepant, can minimize the number of factors that affect the stochastic processes of the stations that will

be used in tectonic and geodynamic studies.

The model that includes flicker noise, in addition to having already been indicated as more suitable for the RBMC, considers that the stations are subject, as a whole, to a common physical base, which may be affected by different seasonal phenomena, such as atmospheric and hydrological loads, atmospheric noise and/or second-order ionospheric effects (Dong et al., 2002; Kedar et al., 2003; Williams et al., 2004).

The WN+RW magnitudes averaged 5.79, 6.23 and $14.65 \text{mm year}^{-\frac{1}{2}}$ in the northern, eastern and up components, respectively (Figure 3). These results agree with values presented in previous works, where the horizontal components are less noisy than the vertical ones (Mao et al., 1999; Langbein, 2004; Amagua et al., 2018).

Figure 4 shows the GNSS stations where at least one component of the noise magnitude was higher than statistically established, in addition to those where at least one component had the index $k < -1$. Of the stations whose k index was lower than -1, only the BRFT station was not classified as an outlier in the GESD test.

Considering that white, flicker and random walk noises predominate in the high, intermediate and low frequencies of the power spectrum of the time series, respectively, we notice the presence of such noises in the 11 stations presented in Figure 4 (referred to as unstable from now on). Figure 5 shows this behavior, in which the signal power density, from a period of approximately 10^3 days, corresponds to the random walk. This result also evidences that a long observation period is necessary to characterize this type of noise. The northern component of the SALU station clearly illustrates the predominance of each type of noise in the power spectrum of the time series, as mentioned previously.

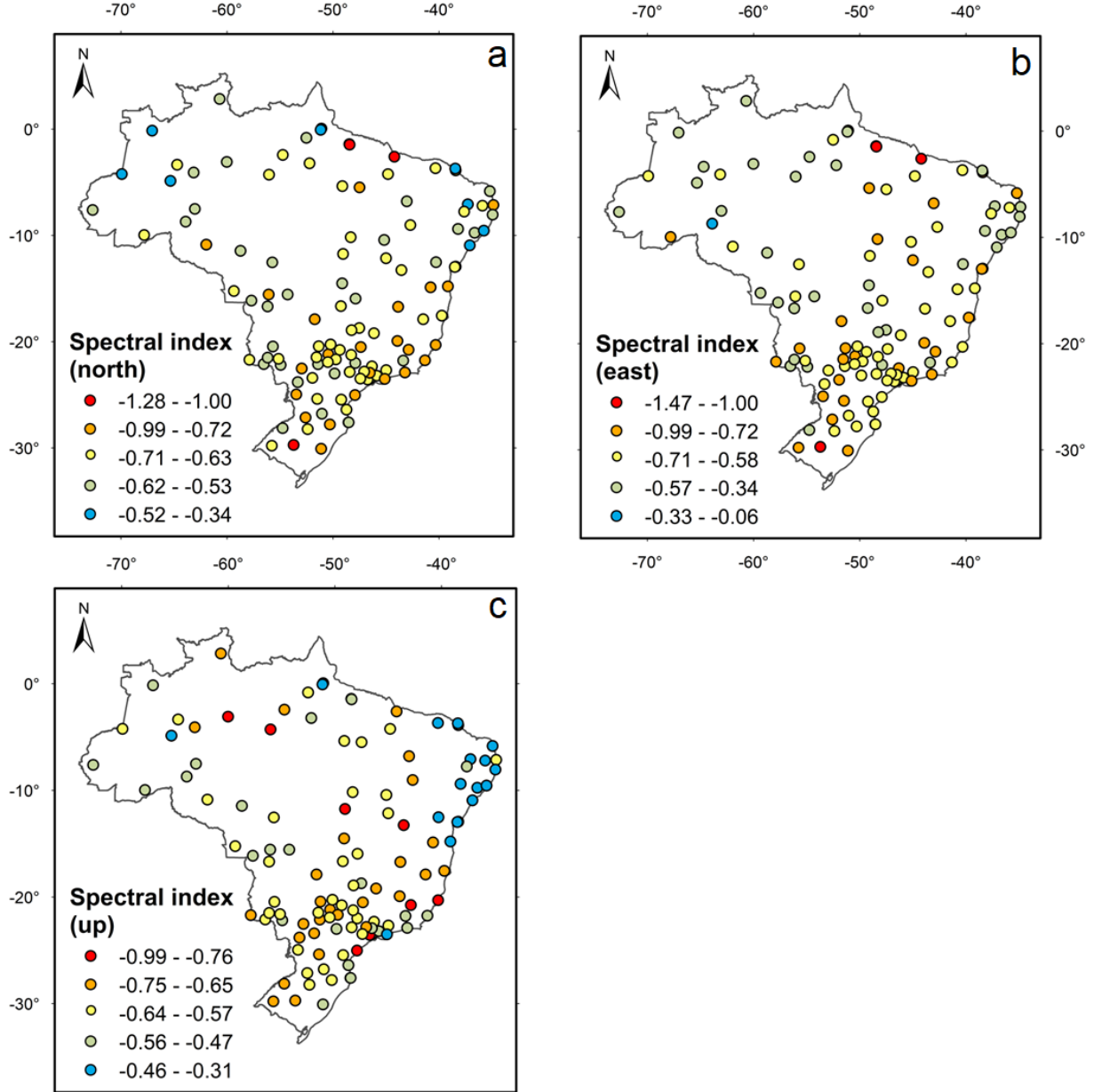


Figure 2: Spectral index of GNSS stations in the north (a), east (b) and up (c) components.

Table 2: Noise amplitude of stations with a spectral index lower than -1 in at least one component. RW+WN express the combined random walk and white noise model. FN+WN refer to the combined white noise and flicker noise model.

Station	RW+WN ($\text{mm} \times \text{year}^{-1/2}$)			FN+WN ($\text{mm} \times \text{year}^{-1/2}$)		
	North	East	Up	North	East	Up
BEPA	20.66	26.12	12.05	9.48	10.27	11.72
BRFT	8.33	4.67	8.45	6.15	3.85	9.55
SALU	16.59	35.10	30.67	7.96	12.71	18.32
SMAR	28.19	46.97	19.96	10.12	11.93	15.95

Table 3: Noise amplitudes classified by GESD (Generalized Extreme Studentized Deviation) as outliers in the north, east and/or up components.

Station	North ($\text{mm} \times \text{year}^{-1/2}$)	East ($\text{mm} \times \text{year}^{-1/2}$)	Up ($\text{mm} \times \text{year}^{-1/2}$)
BEPA	20.66	26.12	—
MGIN	—	8.84	—
NEIA	—	—	42.63
PIFL	—	9.68	—
POLI	—	—	66.38
PRCV	9.09	—	—
SALU	16.59	35.10	30.67
SCCH	12.70	15.55	—
SMAR	28.19	46.97	—
VICO	9.30	11.16	—

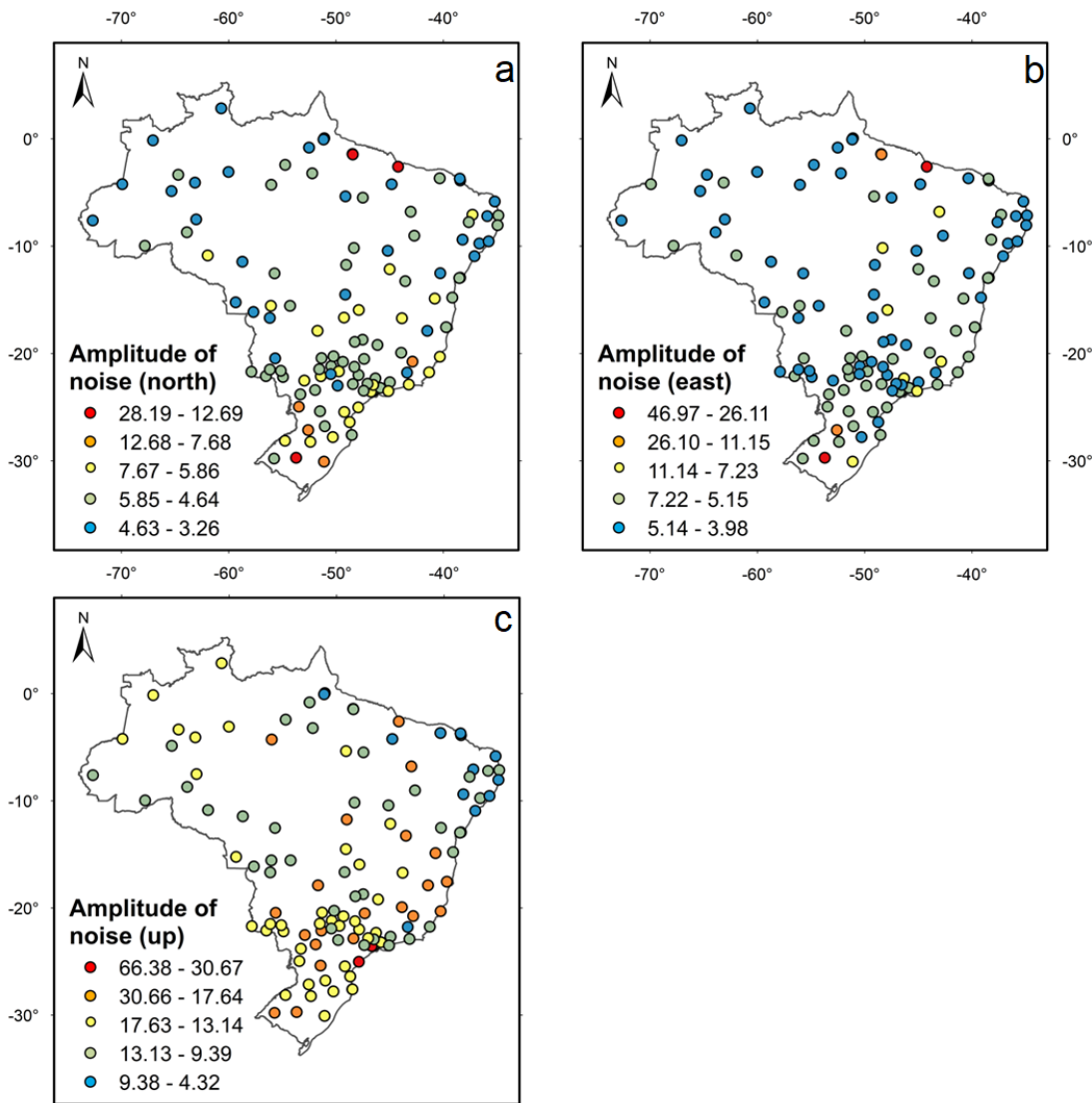


Figure 3: WN+RW noise amplitude, expressed as $\text{mm} \times \text{year}^{-1/2}$, in the north (a), east (b) and up (c) components.

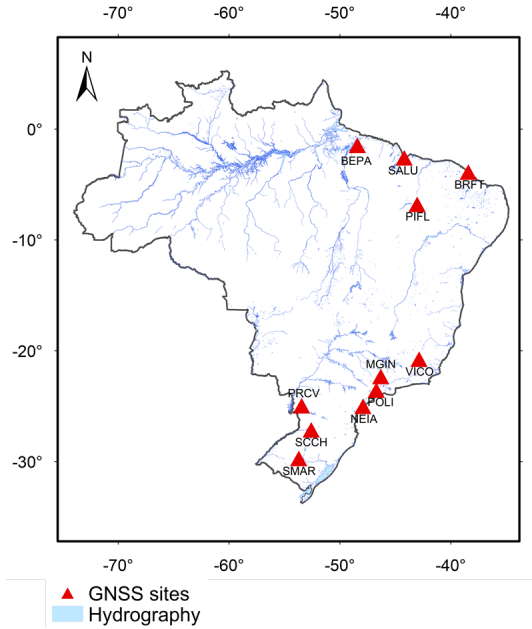


Figure 4: GNSS stations with spectral index or noise amplitude above the limits established for classification of monument stability.

A total of 11 stations present noise magnitude greater than the statistically established value, or with a spectral index $k < -1$ (unstable), of which 4 are either in coastal areas or river basins (Figure 4). These data corroborate previous results presented by [Amagua et al. \(2018\)](#), who stated that the stochastic properties of the time series of these stations may be influenced by typical signals from these locations, such as the effects of hydrological loads. The POLI station, with more than 16 years of observation, is located approximately 500 m from the Pinheiros River and is installed on a building slab and may be subject to various effects that cause instability.

[Ferreira et al. \(2022\)](#) conducted a study in Manaus, AM, and observed annual variations of about 5 meters in the groundwater level and suggested that this is the main source of local variations in the gravity signal. The station studied by the authors has several similarities with the stations classified as unstable in this study, such as being located in thick sedimentary basins, presenting unconsolidated sediments where the geodetic monument is located and being close to rivers whose water levels vary widely.

Thus, it is possible to suggest that both results of the BEPA station, located in the Amazon hydrographic basin, and the BRFT, SALU and NEIA stations, located in coastal areas, can be influenced by local variations in the water level present in the soils and rocks.

The other 6 stations classified as unstable (MGIN, PIFL, PRCV, SCCH, SMAR and VICO) have at least 9 years of observation each. One hypothesis for identifying the instability of these stations is that the longer the observation time, the greater the possibility of identifying random walk noise. Also, more than 70%

of the stations classified as unstable are located in oxisols or argisols (Table 4). Despite being deep soils, which could contribute to the instability of the station, 58% of the national territory is covered by these soil types ([Santos et al., 2018](#)); therefore, it is not possible to directly correlate the soil type with the instability of these stations.

Table 4 shows the distribution of the 11 stations regarding the monument type. The data show that the 7 stations classified as unstable have monument type “concrete pillar on a building slab” or “pillar on a concrete base on the ground”. However, it was not possible to correlate noise magnitude with the type of monumentation, since approximately 80% of the stations have these types of monumentation, a value similar to that observed in stations classified as unstable. Therefore, it is suggested that under the conditions presented, the analysis of the spectral index and noise magnitude of each station in the network, individually, tends to be the most appropriate strategy for classifying unstable stations in the Brazilian territory.

Furthermore, the shortest observation time of stations classified as unstable is 8.8 years (BEPA; Table 4). This raises the hypothesis that stations with shorter observation times do not allow to characterize the random walk appropriately, due either to the magnitude of white and flicker noise or other factors. [Klos et al. \(2018\)](#) identified that the noise character becomes more important than seasonal signals after 9 years of continuous observations. In this case, it is suggested that, for application in geodynamic and tectonic studies, the minimum observation time of 9 years for the RBMC should be considered to be able to identify and classify the different types of noise.

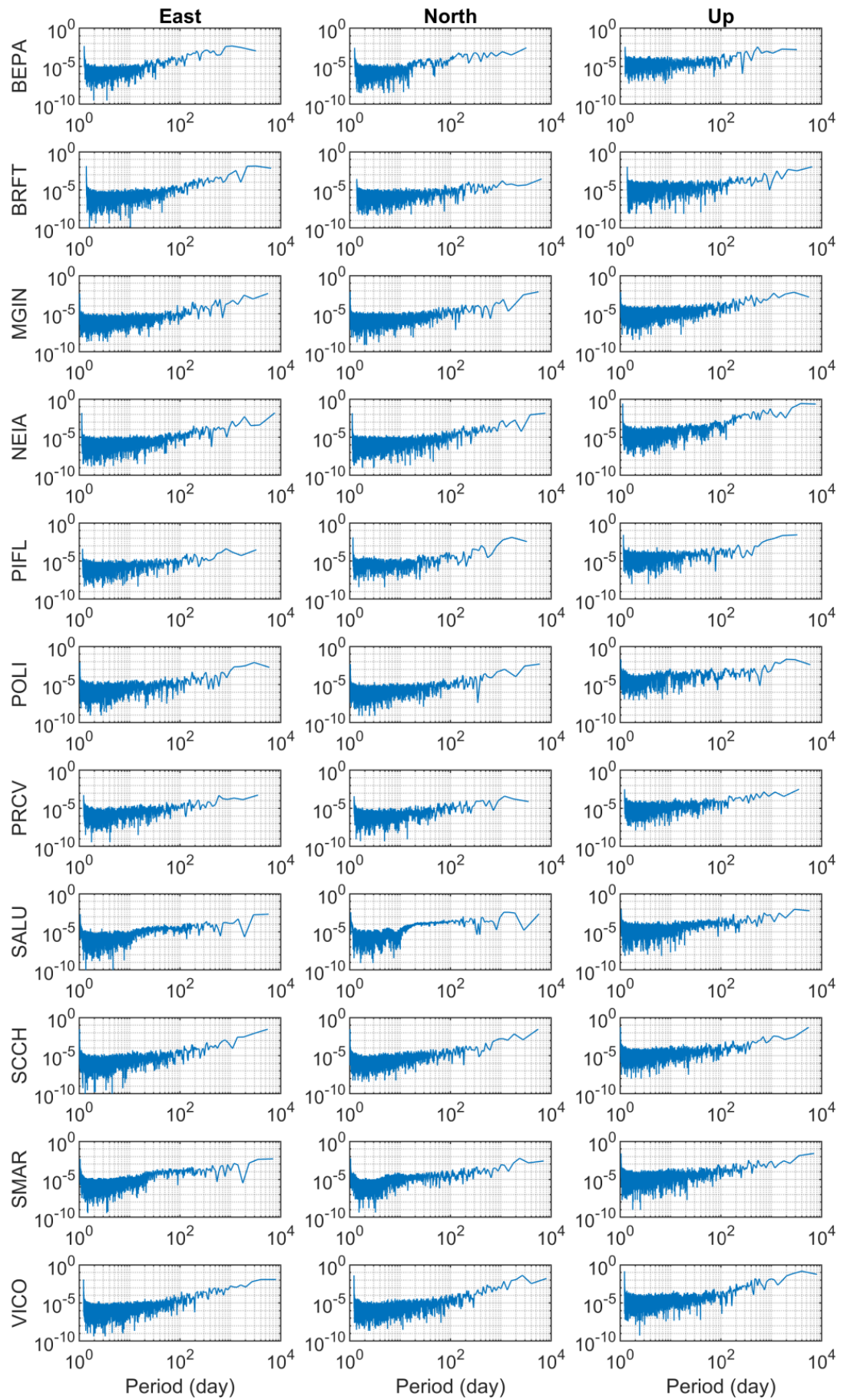


Figure 5: Power spectrum of the time series of the 11 unstable stations.

Table 4: Type of soil, monuments and observation time for removed stations. PBCS = Pillar on a concrete base on the ground. TMLE = Metal tripod on a concrete slab of a building roof. PCLE = Concrete column on a building slab. TMS = Metallic tower on the ground.

Station	Soil	Monumentation	Observation time (years)
BEPA	Gleysol	TMLE	8.80
BRFT	Argisol	PBCS	17.63
MGIN	Oxisol	PCLE	15.33
NEIA	Cambisol	PCLE	20.85
PIFL	Argisol	PBCS	9.00
POLI	Argisol	TMS	16.20
PRCV	Oxisol	TMS	9.70
SALU	Oxisol	PCLE	15.70
SCCH	Neosol	PBCS	15.10
SMAR	Argisol	PCLE	19.34
VICO	Oxisol	PCLE	22.03

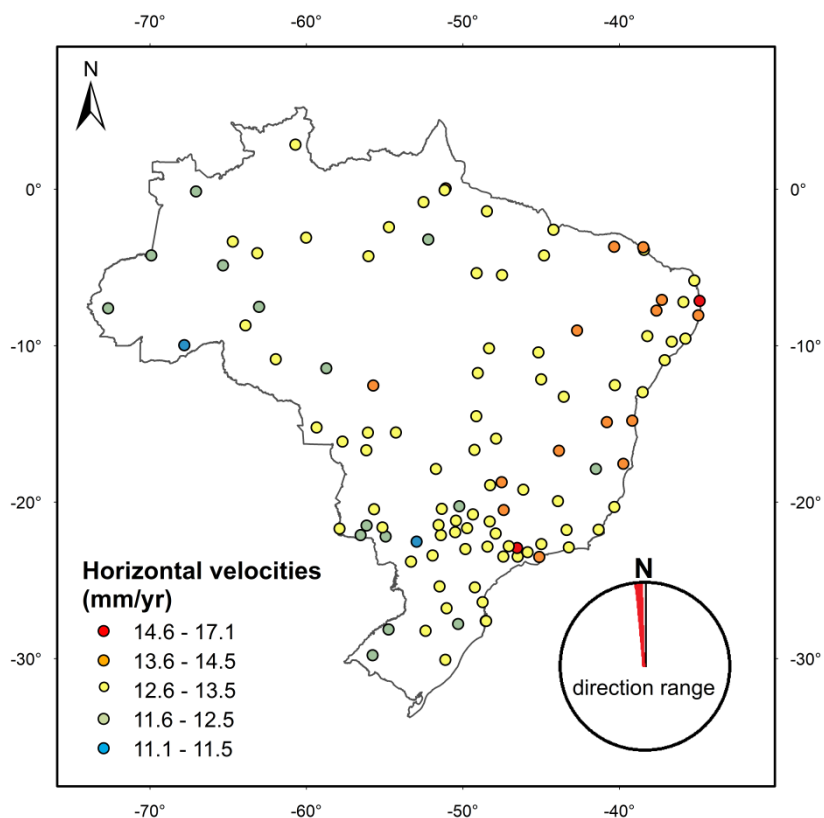


Figure 6: GNSS horizontal velocity model. The noise model used combines white noise and flicker noise.

Figure 6 presents the estimated horizontal velocities model for the stations, considering the noise model that combines white and flicker noises. The average velocities are 13 mm/year, with a standard deviation of 0.7 mm/year. The average velocities of the horizontal components are 12 mm/year in the northern and -3 mm/year in the eastern components and standard deviations of 0.6 and 0.7 mm/year, respectively.

These velocities show that the South American intraplate is in fact stable, which can also be observed in other previously velocity models (e.g., Marotta et al., 2013b; Ramos et al., 2021). Sánchez and Drewes (2020) identified that the only stable regions in Latin America are the Brazilian, Guiana and Atlantic shields. The fact that the estimated velocities agree in magnitude and direction shows that the regional component of plate movement is predominant. Therefore, for studies of local stresses and strains, it is necessary to remove the regional component and analyze the residual components, which may not be suitable for this purpose, depending on the level of estimated uncertainties.

CONCLUSION

The evaluation of 119 GNSS stations located around the Brazilian territory indicates a significant presence of random walk noise in some of these stations, detected from the analysis of the noise magnitude using a model that combines white noise and random walk and, also, from the analysis of the spectral index of the stations.

However, the analysis of elements such as location and type of geodetic station monuments showed that local factors, known or unknown, individually affect the stability of GNSS stations and, therefore, hinder/hamper the full modeling of the data behavior. Thus, it is suggested that adopting a quantitative strategy for characterizing and removing stations considered unstable can provide better quality for tectonic and geodynamic studies.

Regarding the stations where instability of the geodetic monument was identified, most of them are in coastal areas or under the influence of large watercourses. In these locations, a variety of factors may be contributing to the instability of the GNSS station, such as, for example, variations in water level, the presence of unconsolidated sediments, or local atmospheric effects.

Additionally, since the stations with detected instability of the monument cover an observation period of at least eight years, and the identification of the random walk noise depends on the amount of data, it may be suggested that the stations with an observation period between three and eight years may also have been affected by this type of noise, as it was not characterized properly due to the inadequate length

of the time series. In conclusion, we suggest that, in tectonic and/or geodynamic applications, only stations with more than 9 years of observation should be used in Brazil.

REFERENCES

Agnew, D. C., 1992, The time-domain behavior of power-law noises: *Geophysical Research Letters*, **19**, 333–336, doi: [10.1029/91GL02832](https://doi.org/10.1029/91GL02832).

Agurto-Detzel, H., M. Assumpção, C. Ciardelli, D. F. Albuquerque, L. V. Barros, and G. S. L. França, 2014, The 2012–2013 montes claros earthquake series in the São Francisco craton, Brazil: new evidence for non-uniform intraplate stresses in mid-plate South America: *Geophysical Journal International*, **200**, 216–226, doi: [10.1093/gji/ggu333](https://doi.org/10.1093/gji/ggu333).

Amagua, C. G. P., C. P. Krueger, and A. R. T. Criollo, 2018, Stochastic model of the Brazilian GPS network coordinates time series: *Boletim de Ciências Geodésicas*, **24**, 545–563.

Assumpção, M., F. L. Dias, I. Zevallos, and J. B. Naliboff, 2016, Intraplate stress field in South America from earthquake focal mechanisms: *Journal of South American Earth Sciences*, **71**, 278–295, doi: [10.1016/j.jsames.2016.07.005](https://doi.org/10.1016/j.jsames.2016.07.005).

Assumpção, M., M. Schimmel, C. Escalante, J. R. Barbosa, M. Rocha, and L. V. Barros, 2004, Intraplate seismicity in SE Brazil: stress concentration in lithospheric thin spots: *Geophysical Journal International*, **159**, 390–399, doi: [10.1111/j.1365-246X.2004.02357.x](https://doi.org/10.1111/j.1365-246X.2004.02357.x).

Barros, L. V., M. Assumpção, R. Quinteros, and D. Caixeta, 2009, The intraplate Porto dos Gaúchos seismic zone in the Amazon craton, Brazil: *Tectonophysics*, **469**, 37–47, doi: [10.1016/j.tecto.2009.01.006](https://doi.org/10.1016/j.tecto.2009.01.006).

Blewitt, G., W. C. Hammond, and C. Kreemer, 2018, Harnessing the GPS data explosion for interdisciplinary science: *Eos*, **99**, doi: [10.1029/2018EO104623](https://doi.org/10.1029/2018EO104623).

Blewitt, G., and D. Lavallée, 2002, Effect of annual signals on geodetic velocity: *Journal of Geophysical Research*, **107**, 21–45, doi: [10.1029/2001JB000570](https://doi.org/10.1029/2001JB000570).

Bock, Y., S. Wdowinski, P. Fang, J. Zhang, S. Williams, H. Johnson, J. Behr, J. Genrich, J. Dean, M. van Domselaar, D. Agnew, F. Wyatt, K. Stark, B. Oral, B. Hudnut, R. King, T. Herring, S. Dinnardo, W. Young, D. Jackson, and W. Gurtner, 1997, Southern California permanent GPS geodetic array: Continuous measurements of the regional crustal deformation between the 1992 Landers and 1994 Northridge earthquakes: *Journal of Geophysical Research*, **102**, 18013–18033.

Calais, E., J. Y. Han, C. DeMets, and J. M. Nocquet, 2006, Deformation of the North American plate interior from a decade of continuous GPS measurements: *Journal of Geophysical Research*, **111**, B06402, doi: [10.1029/2005JB003870](https://doi.org/10.1029/2005JB003870).

10.1029/2005JB004253.

Cenni, N., E. Mantovani, P. Baldi, and M. Viti, 2012, Present kinematics of central and northern italy from continuous gps measurements: *Journal of Geodynamics*, **58**, 62–72, doi: [10.1016/j.jog.2012.02.004](https://doi.org/10.1016/j.jog.2012.02.004).

Chimpliganond, C. N., M. Assumpção, M. G. von Huelsen, and G. S. França, 2010, The intracratonic caraíbas–itacarambi earthquake of december 09, 2007 (4.9 mb), minas gerais state, brazil: *Tectonophysics*, **480**, 48–56.

Dmitrieva, K., P. Segall, and A. M. Bradley, 2016, Effects of linear trends on estimation of noise in gnss position time-series: *Geophysical Journal International*, **208**, 281–288, doi: [10.1093/gji/ggw391](https://doi.org/10.1093/gji/ggw391).

Dong, D., P. Fang, Y. Bock, M. K. Cheng, and S. Miyazaki, 2002, Anatomy of apparent seasonal variations from gps-derived site position time series: *Journal of Geophysical Research*, **107**, 2075, doi: [10.1029/2001JB000573](https://doi.org/10.1029/2001JB000573).

Farolfi, G., and C. Ventisette, 2015, Contemporary crustal velocity field in alpine mediterranean area of italy from new geodetic data: *GPS Solutions*, doi: [10.1007/s10291-015-0481-1](https://doi.org/10.1007/s10291-015-0481-1).

Ferreira, L., G. S. Marotta, and E. H. Madden, 2022, Hydrological influence on the variation of the terrestrial gravity field in manaus, amazonas, brazil: *Journal of Applied Geophysics*, **206**, 104780, doi: [10.1016/j.jappgeo.2022.104780](https://doi.org/10.1016/j.jappgeo.2022.104780).

Ferreira, V. G., C. E. Ndehedehe, H. C. Montecino, B. Yong, P. Yuan, A. Abdalla, and A. S. Mohammed, 2019, Prospects for imaging terrestrial water storage in south america using daily gps observations: *Remote Sensing*, **11**, doi: [10.3390/rs11060679](https://doi.org/10.3390/rs11060679).

Galloway, D., and D. R. Jones, 1999, Land subsidence in the united states: Circular 1182, U.S. Geological Survey, Reston, VA, USA.

Kedar, S., G. A. Hajj, B. D. Wilson, and M. B. Heflin, 2003, The effect of the second order gps ionospheric correction on receiver positions: *Geophysical Research Letters*, **30**, 1829, doi: [10.1029/2003GL017639](https://doi.org/10.1029/2003GL017639).

Kierulf, H. P., H. Steffen, V. R. Barletta, M. Lidberg, J. Johansson, O. Kristiansen, and L. Tarasov, 2021, A gnss velocity field for geophysical applications in fennoscandia: *Journal of Geodynamics*, **146**, doi: [10.1016/j.jog.2021.101845](https://doi.org/10.1016/j.jog.2021.101845).

Klos, A., G. Olivares, F. N. Teferle, A. Hunegnaw, and J. Bogusz, 2018, On the combined effect of periodic signals and colored noise on velocity uncertainties: *GPS Solutions*, **22**, doi: [10.1007/s10291-017-0674-x](https://doi.org/10.1007/s10291-017-0674-x).

Langbein, J., 2004, Noise in two-color electronic distance meter measurements revisited: *Journal of Geophysical Research: Solid Earth*, doi: [10.1029/2003JB002819](https://doi.org/10.1029/2003JB002819).

Lima, C. C., 2000, Ongoing compression across intraplate south america: observations and some implications for petroleum exploitation and explo- ration: *Revista Brasileira de Geociências*, **30**, 203–207.

Mandelbrot, B., 1983, *The fractal geometry of nature*: W. H. Freeman.

Mao, A., C. G. A. Harrison, and T. H. Dixon, 1999, Noise in gps coordinate time series: *Journal of Geophysical Research*, **104**, 2797–2816.

Marotta, G. S., G. S. França, J. F. G. Monico, F. H. R. Bezerra, and R. A. Fuck, 2015, Strain rates estimated by geodetic observations in the boreborema province, brazil: *Journal of South American Earth Sciences*, **58**, 1–8.

Marotta, G. S., G. S. França, J. F. G. Monico, and R. A. Fuck, 2013a, Strains arising by seismic events in the sirgas-con network region: *Journal of Geodetic Science*, **3**, 12–21.

Marotta, G. S., G. S. França, J. F. G. Monico, R. A. Fuck, and J. O. d. Araújo-Filho, 2013b, Strain rate of the south american lithospheric plate by sirgas-con geodetic observations: *Journal of South American Earth Sciences*, **47**, 136–141, doi: [10.1016/j.jsames.2013.07.004](https://doi.org/10.1016/j.jsames.2013.07.004).

Nikolaidis, R., 2002, Observation of geodetic and seismic deformation with the global positioning system: PhD thesis, University of California, San Diego.

Norabuena, E., L. Leffler-Griffin, A. Mao, T. Dixon, S. Stein, I. S. Sacks, L. Ocola, and M. Ellis, 1998, Space geodetic observations of nazca–south america convergence across the central andes: *Science*, **229**.

Ramos, M. P., W. R. Dal Poz, and A. S. Carvalho, 2021, Determinação de velocidades das estações da rbmc com uso do software sari: *Revista Brasileira de Cartografia*, **73**, 453–469, doi: [10.14393/rbcv73n2-55466](https://doi.org/10.14393/rbcv73n2-55466).

Ramos, M. P., W. R. Dal Poz, and A. S. Carvalho, 2022, Propagação de incertezas no processo de compatibilização de referenciais e época de coordenadas gnss: *Revista Brasileira de Cartografia*, **74**, 305–321, doi: [10.14393/rbcv74n2-64767](https://doi.org/10.14393/rbcv74n2-64767).

Rocha, M. P., P. A. Azevedo, G. S. Marotta, M. Schimmel, and R. A. Fuck, 2016, Causes of intraplate seismicity in central brazil from travel time seismic tomography: *Tectonophysics*, **680**, 1–7, doi: [10.1016/j.tecto.2016.05.005](https://doi.org/10.1016/j.tecto.2016.05.005).

Rosner, B., 1983, Percentage points for a generalized esd many-outlier procedure: *Technometrics*, **25**, 165–172.

Sánchez, L., and H. Drewes, 2020, Geodetic monitoring of the variable surface deformation in latin america, in *Beyond 100: The Next Century in Geodesy*: Springer, volume **152** of International Association of Geodesy Symposia. doi: [10.1007/1345_2020_91](https://doi.org/10.1007/1345_2020_91).

Santos, H., P. Jacomine, L. Anjos, V. Oliveira, J. Lumbreiras, M. Coelho, J. Almeida, J. Araújo Filho, J. Oliveira, and T. Cunha, 2018, *Sistema brasileiro de classificação de solos*, 5 ed.: Embrapa.

Williams, S. D. P., 2008, Cats: Gps coordinate time series analysis software: GPS Solutions, **2**, 147–153, doi: [10.1007/s10291-007-0086-4](https://doi.org/10.1007/s10291-007-0086-4).

Williams, S. D. P., Y. Bock, P. Fang, P. Jamason, R. M. Nikolaidis, L. Prawirodirdjo, M. Miller, and D. J. Johnson, 2004, Error analysis of continuous gps position time series: Journal of Geophysical Research, **109**, B03412, doi: [10.1029/2003JB002741](https://doi.org/10.1029/2003JB002741).

Wyatt, F. K., 1989, Displacements of surface monuments: Vertical motion: Journal of Geophysical Research, **94**, 1655–1664.

Yadav, R., and V. M. Tiwari, 2018, Numerical simulation of present-day tectonic stress across the indian subcontinent: International Journal of Earth Sciences, **107**, 2449–2462, doi: [10.1007/s00531-018-1607-9](https://doi.org/10.1007/s00531-018-1607-9).

Almeida, Y.M.: conceptualization, methodology, writing – original draft, formal analysis; **Marotta, G.S.:** conceptualization, methodology, writing – original draft, formal analysis, supervision; **Monico, J.F.G.:** writing – review editing; **Brassarote, G.O.N.:** writing – review editing; **França, G.S.A.:** writing – review editing.

Received on February 22, 2024 / Accepted on June 26, 2024



Creative Commons attribution-type CC BY